

Nonlinear mirror based on cross-polarized wave generation

S. Kourtev, N. Minkovski, and S. M. Saltiel

Faculty of Physics, University of Sofia, 5 J. Bourchier Boulevard, BG-1164, Sofia, Bulgaria

A. Jullien, O. Albert, and J. Etchepare

Laboratoire d'Optique Appliquée, UMR 7639 CNRS, Ecole Polytechnique, Ecole Nationale Supérieure de Techniques Avancées, 91761 Palaiseau cedex, France

Received April 27, 2006; revised July 24, 2006; accepted August 9, 2006;
posted August 23, 2006 (Doc. ID 70403); published October 11, 2006

We present a new type of nonlinear mirror based on the generation of a cross-polarized wave through a nonresonant electronic third-order process. It is characterized by a reflection coefficient that depends on the input intensity. Its behavior results from the interference between the nonlinearly generated cross-polarized wave and a $\pi/2$ phase-retarded wave. This setup has a lot of advantages: it does not require any phase matching, it is achromatic and suitable for femtosecond pulses, linear losses are easily adjustable, and the overall behavior is predictable. The device has been experimentally tested using BaF₂ and YVO₄ crystals.

© 2006 Optical Society of America

OCIS codes: 190.0190, 230.4320, 140.4050.

Nonlinear mirrors (NLMs) are known to be used for mode-locking (ML) operation in solid-state lasers and also for other applications, e.g., for pulse reshaping and compression and contrast improvement. In general, NLMs can be divided into two groups. The first group is based on $\chi^{(3)}$ effects: self-induced ellipse rotation in isotropic media,^{1,2} the Kerr lens effect,³ or interference effects in an external cavity with $\chi^{(3)}$ media.⁴ The second group uses second-harmonic generation in quadratic crystals and involves $\chi^{(2)}$: $\chi^{(2)}$ cascaded processes.^{5–8} The requirement of phase matching reduces, in this last case, the ability of such a mirror for ML in the femtosecond regime because of the unavoidable group velocity dispersion. Therefore in the femtosecond regime, ML based on nonresonant $\chi^{(3)}$ effects (self-focusing or external cavity ML^{3,4,9–11}) has been proved to be an efficient method. We recall that semiconductor saturable absorber mirrors are also frequently used for ML lasers in the near-infrared region.¹²

Here, we introduce a new type of NLM based on the generation of a linearly polarized wave cross polarized to the input one. The cross-polarized wave (XPW) generation effect is a four-wave mixing process that depends on the anisotropy of the $\chi^{(3)}$ tensor.^{13,14} In contrast to self-induced ellipse rotation, the process of XPW generation cannot be realized in $\chi^{(3)}$ -isotropic media. As shown recently, the efficiency of XPW generation in a single crystal can reach more than 10%,^{15,16} which allows for a reasonable reflection dynamics usable in a NLM. The device we describe in this Letter has an intensity-dependent reflection coefficient (RC) and is moreover insensitive to group velocity dispersion. We believe that it can find applications for ML of solid-state lasers as well as for optical manipulation of fs pulses.

The scheme of the XPW-based NLM is shown in Fig. 1. The laser pulses are issued from a colliding pulse ML dye laser (used maximum energy, 10 μ J;

duration, 100 fs; frequency, 10 Hz; wavelength, 620 nm). The setup consists of a nonlinear crystal (NLC) located at a focal plane defined on one side by a lens ($f=30$ cm) and on the other side by a concave mirror ($R=40$ cm). The quarter-wave plate (QWP) and the NLC were uncoated. The NLM works as follows. At very low intensity, the crystal does not generate any XPW, and the reduced reflectivity of the system results from the rotation of the QWP by an

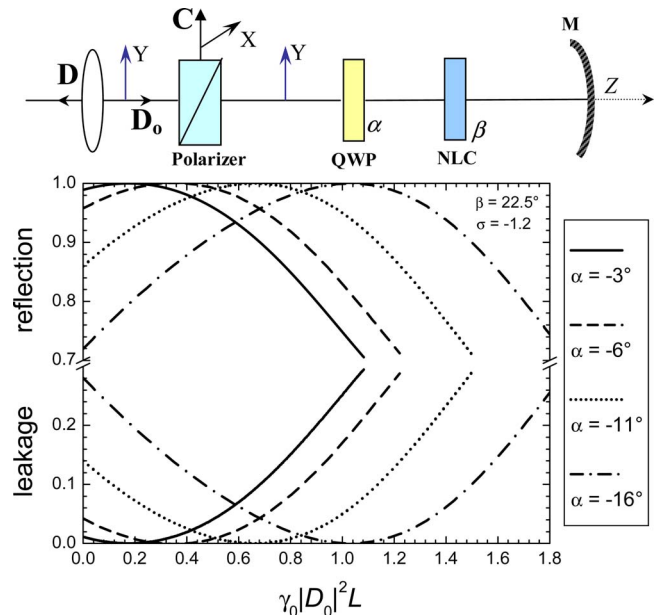


Fig. 1. (Color online) (a) Schematic of the NLM-XPW experiment. D_0 , input beam; D , reflected beam; C , leakage beam (losses); NLC, nonlinear crystal; M, maximum reflectivity concave mirror; QWP, quarter-wave plate. The QWP and the NLC can both be rotated, respectively, by α and β angles around the propagation axis. (b) Top curves: intensity reflection coefficient of the NLM-XPW. Bottom curves: intensity leakage coefficient. The angle $\beta = 22.5^\circ + \alpha$.

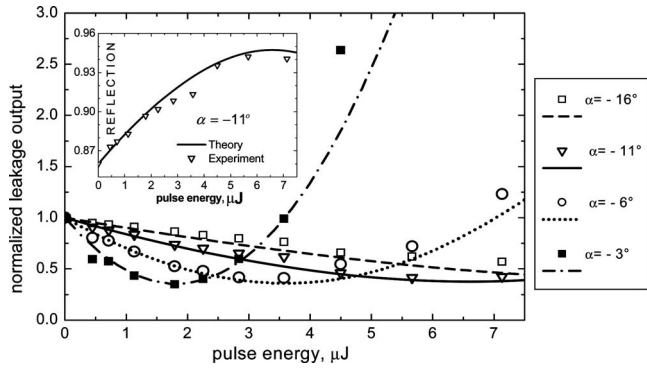


Fig. 2. Measured energy leakage coefficient (points) of NLM-XPW with BaF₂ and theoretical predictions (curves) obtained assuming Gauss temporal and spatial shape. The leakage coefficient is normalized to the linear (low-intensity) losses. The angle $\beta = 22.5^\circ + \alpha$. The fit is obtained by the rescaling of $S = \gamma_0 |D_o|^2 L$. For this fit, the 1 μJ pulse energy corresponds to $S = 0.175$. The inset shows the recalculated RC for $\alpha = -11^\circ$.

angle α (α is the angle between the QWP axis and the input polarization direction). After a double pass through the QWP, the polarization of the reflected wave is rotated by an angle of 2α , and the leakage and reflected beams after the polarizer have squared amplitudes: $|C|^2 = |D_o|^2 (\sin 2\alpha)^2$ and $|D|^2 = |D_o|^2 (\cos 2\alpha)^2$. The linear losses are then $M = |C|^2 / |D_o|^2 = (\sin 2\alpha)^2$. At a higher intensity, the NLC generates a XPW. The elliptical light after the QWP can be equivalently considered as two waves lying in perpendicular polarization planes: (i) the fundamental wave (FW), and (ii) the seeding wave that is $\pi/2$ phase shifted with respect to the FW. The amplitudes of these two waves at the input of the NLC are $A_o = D_o \cos \alpha$ (big axis) and $B_o = D_o \sin \alpha$ (small axis). The XPW generated in the NLC with amplitude B is also phase shifted by $\pi/2$ with respect to the FW.¹⁴ Its amplitude is governed by the nonlinear coefficient γ_\perp , whose sign depends on the β angle value through $\gamma_\perp = -\gamma_o (\sigma/4) \sin(4\beta)$; σ is the $\chi^{(3)}$ tensor/anisotropy, and $\gamma_o = (6\pi/8\lambda n) \chi_{xxxx}^{(3)}$. The seeding wave B_o and the generated XPW B are in phase, and they interfere constructively or destructively, depending on β and α relative values. The system can work as a NLM suitable for ML when losses introduced by the QWP are decreasing, while the intensity increases. For this purpose, the seeding wave and the XPW fields have to be of opposite sign. The reflected beam amplitude can in this case be written as $D = [B(2L) - B_o] \sin \alpha + A_o \cos \alpha$, and equivalently, the leakage beam amplitude is written as $C = [B(2L) - B_o] \cos \alpha - A_o \sin \alpha$, where L is the length of the NLC. For an input intensity that leads to $[B(2L) - B_o] = B_o$, the RC will be 100%, and no leakage beam will appear. The above considerations do not include the depletion of the FW; they nevertheless perfectly explain the mechanism of nonlinear behavior of the RC. As shown below, the FW depletion does not change the behavior of the NLM-XPW, and intensity values for which the RC is 100%, i.e., the leakage is zero, also exist in this regime.

The numerical solution of the system of coupled differential equations described in Ref. 17, which takes into account the depletion of the FW and the effects of self- and cross-phase modulation, leads to the behavior illustrated in Fig. 1(b). We demonstrated that at each value of angle α , which defines the static losses, an $S = \gamma_0 |D_o|^2 L$ value can be obtained for which overall losses turn out to be zero, and the NLM reflection recovers its maximum 100% value. We name gate intensity the intensity that corresponds to this maximum in RC. In case the input radiation has some temporal and spatial distribution, the curves shown in Fig. 1(b) relate to the peak intensity of the reflected pulses (since plane-wave approximation is used). The integration of the plane-wave solution in space and time will lead to an energy reflection that is always < 1 and energy leakage higher than zero as illustrated in Fig. 2. The RC of the peak intensity shown in Fig. 1(b) is, however, the parameter of prime importance for ML purposes.

For NLM experimental characterization, we measured the energy of the leakage beam versus the input energy and angle β for different values of the angle α . To obtain a representation of these dependencies independently from the reflection losses, including those from the optical elements used in the experiment, the leakage coefficient has been normalized with respect to its value at a very small input energy. This value has been measured by locating the NLC far from the focal spot, i.e., very close to the folding mirror.

The experimental results, obtained using a 0.9 mm long BaF₂ crystal, are shown in Figs. 2 and 3. The only parameter used to fit the theoretical curves to the experimental ones is a scaling factor that links measured pulse energy to the S value. It is seen that for each α , an optimum energy exists for which the losses are minimal, and consequently, the energy RC of NLM is maximum. We define this value of the energy as the gate energy W_{gate} . For example, for $\alpha = -6^\circ$, the gate energy is $W_{\text{gate}} \approx 3.6 \mu\text{J}$. The W_{gate} can be lowered in different ways: by choosing a smaller α value, a longer crystal length, stronger focusing, or a crystal having higher nonlinear parameters.

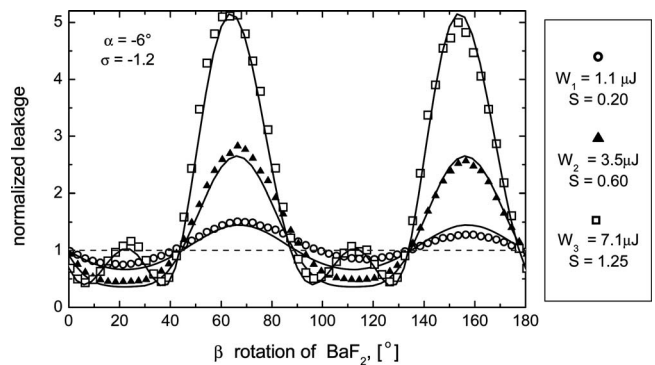


Fig. 3. Measured energy leakage coefficient (points) of the NLM-XPW with BaF₂ normalized to the linear losses as a function of angle β (with $\alpha = -6^\circ$). The curves are the theoretical predictions that take into account the Gaussian spatial and the temporal shape of the beam.

γ_{\perp} dependence on angle β can furthermore be used to obtain a better insight into the NLM properties. The leakage energy normalized to the linear (low-intensity) losses is shown in Fig. 3 as a function of the angle β . The dashed horizontal line corresponds to extremely small energies where the leakage is equal to the linear losses. For $W=W_1 < W_{\text{gate}}$, the generated XPW signal $B(2L)$ has a smaller amplitude than the seeding signal B_o , and as a result of the interference, the leakage energy is oscillating around the value of linear losses following the change of the value and sign of γ_{\perp} as a function of β . For $W=W_2 = W_{\text{gate}}$, the leakage energy is minimized, and consequently, the RC is periodically maximized at angles $\pi/8 + m\pi/2$. For $W=W_3 > W_{\text{gate}}$, the XPW signal $B(2L) > B_o$ and the process of XPW generation is attempting to recover its $\pi/4$ periodicity whatever the introduced linear losses are. It is evident from Fig. 3 that the leakage has a minimum, and RC has a maximum for a β range of $\sim 10^\circ$. Therefore the β angle does not primarily determine the amplitude of the RC change, but it influences the slope of this intensity-dependent RC change. Theoretical curves have been plotted without any additional adjustable parameter other than the scaling factor used for Fig. 2. They very nicely describe the experimental results.

We have performed identical experiments using a 0.9 mm long YVO₄ crystal. For $\alpha=6^\circ$, we measured a 5.15 times smaller gate energy: $W_{\text{gate}}(\text{YVO})_4 = 0.7 \mu\text{J}$. The square of this number (26.4) corresponds to a previously measured ratio of $26 \pm 10\%$.¹⁵ From this comparative measurement of W_{gate} in YVO₄ and BaF₂, we conclude that NLM-XPW is also suitable for relative measurements of the $\chi_{\text{xxxx}}^{(3)} \sigma$ product in crystals. This would be a useful technique for testing the potential of crystals for use in contrast enhancement setups based on XPW generation.

The scheme in Fig. 1 has an equivalent analog in the transmission mode where the mirror is changed to a second pair of QWPs and polarizer elements. A transmission mode operation will have the advantage that the output polarizer can be switched between two positions, allowing either intensity-induced transparency or intensity-induced darkening to be obtained.

In conclusion, we have described a new $\chi^{(3)}$ nonlinear device that is based on interference effects using cross-polarized wave generation in crystals as a nonlinear process. One of its potential applications is ML in solid-state lasers. For some ML regimes, decreasing losses of only 1% to 2% can lead to ML. Here, we demonstrate experimentally (see the inset in Fig. 3) that for an 11° rotation angle of QWP, one can regain 90% of the losses inserted by the wave plate. Naturally, at the high intensity required for this device to

work, the effects of self-focusing and self-phase modulation will also take place. In ML applications, the Kerr lens effect can be used together with the XPW effect, or one has to design a resonator that is insensitive to the self-focusing.

Other potential applications include power limiting and cleaning of femtosecond pulses. The main advantages of the NLM based on XPW generation include the freedom to choose any wavelength (inside the transparency region), no phase matching constraint, no group velocity mismatch, and an easy control of linear losses and energy suitable for maximum reflection.

The authors acknowledge the support of the program "Access to Research Infrastructure" contract (LaserLab-Europe, R\|3-CT-2003-506350). N. Minkovski, S. Kourtev, and S. M. Saltiel thank the Bulgarian Science Fund for support with grant 1201/2002. S. Saltiel's e-mail address is saltiel@phys.uni-sofia.bg. S. Kourtev's e-mail address is skourtev@phys.uni-sofia.bg.

References

1. L. Dahlström, *Opt. Commun.* **5**, 157 (1972).
2. K. Sala, M. C. Richardson, and N. R. Isenor, *IEEE J. Quantum Electron.* **QE-13**, 915 (1977).
3. D. E. Spence, P. N. Kean, and W. Sibbett, *Opt. Lett.* **16**, 42 (1991).
4. E. P. Ippen, H. A. Haus, and L. Y. Liu, *J. Opt. Soc. Am. B* **6**, 1736 (1989).
5. K. A. Stankov, *Appl. Phys. B* **45**, 191 (1988).
6. G. I. Stegeman, D. J. Hagan, and L. Torner, *Opt. Quantum Electron.* **28**, 1691 (1996).
7. G. Cerullo, S. De Silvestri, A. Monguzzi, D. Segala, and V. Magni, *Opt. Lett.* **20**, 746 (1995).
8. V. Couderc, F. Louradour, and A. Barthélémy, *Opt. Commun.* **166**, 103 (1999).
9. U. Keller, G. W. 't Hooft, W. H. Knox, and J. E. Cunningham, *Opt. Lett.* **16**, 1022 (1991).
10. F. Salin, J. Squier, and M. Piché, *Opt. Lett.* **16**, 1674 (1991).
11. H. A. Haus, J. G. Fujimoto, and E. P. Ippen, *IEEE J. Quantum Electron.* **28**, 2086 (1992).
12. I. D. Jung, F. X. Kärtner, N. Matuschek, D. H. Sutter, F. Morier-Genoud, Z. Shi, V. Scheuer, M. Tilsch, T. Tschudi, and U. Keller, *Appl. Phys. B* **65**, 137 (1997).
13. Yu. P. Svirko and N. I. Zheludev, *Polarization of Light in Nonlinear Optics* (Wiley, 1998).
14. N. Minkovski, S. Saltiel, G. Petrov, O. Albert, and J. Etchepare, *Opt. Lett.* **27**, 2025 (2002).
15. N. Minkovski, G. Petrov, S. M. Saltiel, O. Albert, and J. Etchepare, *J. Opt. Soc. Am. B* **21**, 1659 (2004).
16. A. Jullien, O. Albert, G. Chériaux, J. Etchepare, S. Kourtev, N. Minkovski, and S. M. Saltiel, *Opt. Express* **14**, 2760 (2006).
17. A. Jullien, O. Albert, G. Chériaux, J. Etchepare, S. Kourtev, N. Minkovski, and S. M. Saltiel, *J. Opt. Soc. Am. B* **22**, 2635 (2005).